Detectability of the gravitational-wave background produced by magnetar giant flares

Nikolaos Kouvatsos[1], Paul D. Lasky[2,3] Ryan Quitzow-James[4] and Mairi Sakellariadou[1]

[1]*Theoretical Particle Physics and Cosmology Group, Physics Department, King's College London,*
University of London, Strand, London WC2R 2LS, United Kingdom
[2]*School of Physics and Astronomy, Monash University,*
Victoria 3800, Australia
[3]*OzGrav: The ARC Centre of Excellence for Gravitational-wave Discovery,*
Clayton, Victoria 3800, Australia
[4]*Institute of Multi-messenger Astrophysics and Cosmology,*
Missouri University of Science and Technology,
Rolla, Missouri 65409, USA

We study the gravitational-wave background produced by f-mode oscillations of neutron stars triggered by magnetar giant flares. For the gravitational-wave energy, we use analytic formulas obtained via general relativistic magnetohydrodynamic simulations of strongly magnetized neutron stars. Assuming the magnetar giant flare rate is proportional to the star-formation rate, we show the gravitational-wave signal is likely undetectable by third-generation detectors such as the Einstein Telescope and Cosmic Explorer. We calculate the minimum value of the magnetic field and the magnetar giant flare rate necessary for such a signal to be detectable, and discuss these in the context of our current understanding of magnetar flares throughout the Universe.

I. INTRODUCTION

Magnetar giant flares (MGFs) are extremely luminous transients arising from violent explosions in the magneto-spheres of strongly magnetized neutron stars known as magnetars. Several such flares have been detected thus far, with tails typically lasting $\sim(200-400)$ s and unleashing $\gtrsim 10^{44}$ erg of energy in hard x-rays and soft gamma rays [1–3]. While this energy is emitted as electromagnetic radiation, MGFs may also lead to the emission of gravitational waves (GWs) via the excitation of oscillation modes inside the neutron stars [4,5]. This has motivated several theoretical and observational studies on the detection of GWs resulting from MGFs [e.g., [6–16]].

Theoretical studies of GWs from MGFs have primarily focused on the f mode [e.g., [5,15–19]], which is considered the most efficient emission mode [20,21]. Some of these works [16,19] performed general relativistic magnetohydromagnetic simulations assuming different polytropic equations of state for neutron star matter showing that the f mode may just be detectable from a Galactic MGF with third-generation gravitational-wave observatories such as the Einstein Telescope (ET) [22] or Cosmic Explorer (CE) [23]. Other oscillation modes, such as Alfvén modes and g modes, may also produce lower frequency GWs, but their contribution is likely small compared to the dominant f mode [24,25].[1]

No evidence of GWs from magnetar short bursts [8,9,26–32] or MGFs [6–12,14] has been found to date.

In this study, we explore the contribution of MGFs to the GW background. Previous studies of the GW background from magnetars have considered the emission of GWs from magnetars due to nonzero stellar ellipticities from internal magnetic fields [e.g., [33–37]]. We follow the same main principles to construct the background, but for the GW energy we consider the excitation of the f mode arising from MGFs using the results of [18] for the GW strain. We obtain a normalized GW energy spectrum for the background from MGFs that we compare with the third-generation (3g) detector sensitivities.

The rest of the paper is organized as follows. In Sec. II, we outline our model used to calculate the GW background. In Sec. III, we obtain the GW energy spectrum of MGFs. Then, in Sec. IV, we examine the detectability of the resulting signal assuming a network consisting of ET and

---

[1]In [16], it is suggested that Alfven modes can be considered to be serious candidates for producing observable GWs, however it is also pointed out that detectability requires a better knowledge of the various damping mechanisms relevant to these modes of oscillation.

CE and place constraints on the minimum required MGF rate and magnetic field strength for detection. We present our conclusions in Sec. V.

II. GW BACKGROUND MODEL

The GW background is described by the normalized GW energy spectrum [38]

$$\Omega_{\mathrm{GW}}(f_{\mathrm{o}}) = \frac{1}{c^2 \rho_{\mathrm{c}}} \frac{\mathrm{d}\rho_{\mathrm{GW}}}{\mathrm{d}\ln f}\bigg|_{f_{\mathrm{o}}}, \quad (1)$$

where $\rho_{\mathrm{c}} = 3H_0^2/(8\pi G)$ is the critical density, H_0 is Hubble's constant, c the speed of light, G Newton's gravitational constant, and f_{o} the emitted GW frequency as measured in the observer frame. For astrophysical sources, Eq. (1) can be rewritten as [34]

$$\Omega_{\mathrm{GW}}(f_{\mathrm{o}}) = \frac{f_{\mathrm{o}}}{c^3 \rho_{\mathrm{c}}} F(f_{\mathrm{o}}), \quad (2)$$

where

$$F(f_{\mathrm{o}}) = \int_0^{z_{\mathrm{max}}} \frac{R_{\mathrm{MGF}}(z)}{4\pi d_c^2(z)} \frac{\mathrm{d}E_{\mathrm{GW}}}{\mathrm{d}f}\bigg|_{f_s} dz, \quad (3)$$

is the integrated flux density, $R_{\mathrm{MGF}}(z)$ is the MGF rate as a function of redshift z, $d_{\mathrm{c}}(z)$ the comoving distance, $\mathrm{d}E_{\mathrm{GW}}/\mathrm{d}f$ the GW energy spectrum, and $f_{\mathrm{s}} = f_{\mathrm{o}}(1 + z)$ the GW frequency in the source frame.

The rate $R_{\mathrm{MGF}}(z)$ can be expressed in terms of the MGF rate per unit comoving volume, $R_{\mathrm{MGF}(V)}(z)$, as

$$R_{\mathrm{MGF}}(z) = \frac{R_{\mathrm{MGF}(V)}(z)}{1 + z} \frac{\mathrm{d}V}{\mathrm{d}z} = \frac{4\pi c}{H_0} \frac{R_{\mathrm{MGF}(V)}(z) d_c^2(z)}{(1 + z)E(z)}, \quad (4)$$

where $E(z) = \sqrt{\Omega_{\mathrm{m}}(1 + z)^3 + \Omega_\Lambda}$, with Ω_{m} and Ω_Λ the energy density of baryonic matter and dark energy, respectively. We adopt a flat ΛCDM model with $\Omega_{\mathrm{m}} = 0.311$, $\Omega_\Lambda = 0.689$ [39] and $H_0 = 67.7$ km/s/Mpc [40]. The $(1 + z)$ in the denominator, Eq. (4), accounts for cosmic expansion.

We obtain the MGF rate assuming a linear scaling with the star formation rate (SFR). We note that there is a delay time between the birth of a star and its evolution into a magnetar. However, since the lifetime of a star (mass from $8\,M_\odot$ to $40\,M_\odot$ [36]) turning into a neutron star is at most of order 10^7 yr [41] and magnetar magnetic fields decay within 10^5 yr [42–47], we deduce that adding a delay time has a negligible impact on our results.

We relate $R_{\mathrm{MGF}(V)}$ to the SFR via a proportionality constant λ:

$$R_{\mathrm{MGF}(V)}(z) = \lambda R_*(z), \quad (5)$$

where

$$R_*(z) = 0.015 \frac{(1 + z)^{2.7}}{1 + [(1 + z)/2.9]^{5.6}} M_\odot \text{ yr}^{-1} \text{ Mpc}^{-3}, \quad (6)$$

denotes the SFR, which is taken up to $z_{\mathrm{max}} = 8$ [48].

We define λ as the proportionality constant that relates the MGF rate to the SFR (we stress that this definition is different from the typical one that exists in the literature [33,36]). It is equal to the mass fraction of stars that is converted into magnetars times the mean number of MGFs per magnetar. We presume that a magnetar will emit a number of MGFs during its lifetime, the value of which is not well known. Assuming that all neutron stars are born as magnetars [49], we consider an upper limit of $0.01 M_\odot^{-1}$ for the mass fraction that is converted into magnetars, following [36]. We then multiply this by the number of MGFs per magnetar to obtain λ. For example, a mean value of 10^2 MGFs per magnetar yields $\lambda = 1 M_\odot^{-1}$, while a value of 10^4 MGFs per magnetar results in $\lambda = 10^2 M_\odot^{-1}$. The authors of Ref. [50] inferred a local (i.e., $z = 0$) volumetric rate $R_{\mathrm{MGF}(V)}(0) = 3.8 \times 10^5$ Gpc^{-3} yr^{-1}. Plugging this value in Eq. (5) and solving for $z = 0$ (today) yields $\lambda = 0.025 M_\odot^{-1}$ [50]. We use this as our reference value for λ, but also explore alternative values to understand the difference it makes on predictions for the stochastic GW background.

Our final expression for the normalized GW energy spectrum then reads:

$$\Omega_{\mathrm{GW}}(f_{\mathrm{o}}) = \frac{\lambda f_{\mathrm{o}}}{\rho_{\mathrm{c}} H_0 c^2}$$

$$\times \int_0^{z_{\mathrm{max}}} \frac{R_*(z) \frac{\mathrm{d}E_{\mathrm{GW}}}{\mathrm{d}f}\big|_{f_s}}{(1 + z)\sqrt{\Omega_{\mathrm{m}}(1 + z)^3 + \Omega_\Lambda}} \, \mathrm{d}z. \quad (7)$$

III. GW ENERGY SPECTRUM

Studies [15,17] estimated the GW energy available to MGFs by considering a catastrophic and instantaneous rearrangement of the internal magnetic field of the star. Later work suggests this provides an overly optimistic estimate, for example the timescale for the rearrangement is long compared to the characteristic f-mode frequency [5]. We therefore utilise more realistic estimates for the GW energy from numerical-relativity simulations. General relativistic magnetohydrodynamic simulations of magnetars designed to mimic the internal magnetic field rearrangement immediately following an MGF show scaling relations between the star's magnetic field strength at the pole B_{pole} (assuming a poloidal configuration for the magnetic field), the emitted gravitational-wave strain in the f mode, and the stellar mass M and radius R [16,18]:
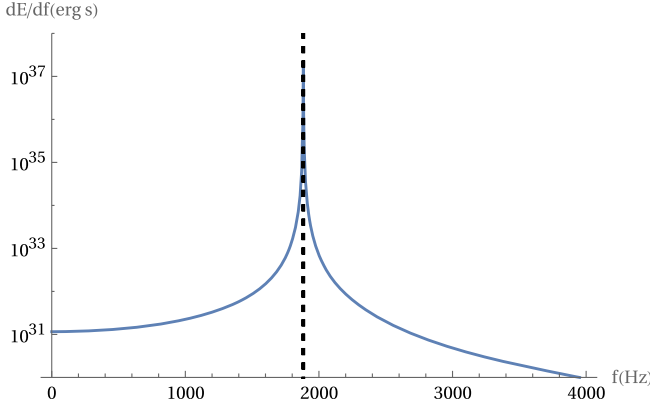
FIG. 1. The GW energy spectrum emitted via a single MGF from a magnetar with $B_{pole} = 10^{15}$ G. Treating the GW strain as an exponentially decaying sinusoid leads to a sharp peak at the f_{fmode} frequency.

$$h_{max} = 8.5 \times 10^{-28}$$
$$\times \frac{10 \text{ kpc}}{d} \left(\frac{R}{10 \text{ km}}\right)^{4.8} \left(\frac{M}{M_\odot}\right)^{1.8} \left(\frac{B_{pole}}{10^{15} \text{ G}}\right)^{2.9}. \quad (8)$$

We model the GW strain as an exponentially decaying sinusoid peaked at the f-mode frequency:

$$h = h_{max} \sin(2\pi f_{fmode}) e^{-\frac{t}{\tau}}, \quad (9)$$

where f_{fmode} is the f-mode frequency and τ is the decay constant. We consider a typical mass $M = 1.4\ M_\odot$ and a radius $R = 13$ km, consistent with [51,52], and a single value of B_{pole} to describe the whole magnetar population in the Universe. The corresponding equation of state yields $f_{fmode} = 1883.1$ Hz and $\tau = 0.25$ s, using [53].

The total GW energy emitted is [5]

$$E_{GW} = \frac{2\pi^2 d^2 f_{fmode}^2 c^3}{G} \int_{-\infty}^{+\infty} |h(t)|^2 dt$$
$$= \frac{2\pi^2 d^2 f_{fmode}^2 c^3}{G} \int_{-\infty}^{+\infty} |\hat{h}(2\pi f)|^2 df, \quad (10)$$

where the second equality comes from Parseval's theorem, and $\hat{h}$ is the Fourier transform of h.[2] We calculate this Fourier transform and take the one-sided energy spectrum to obtain dE_{GW}/df, which we plot in Fig. 1 for $B_{pole} = 10^{15}$ G, a value within the range of the magnetic field strength at the surface of magnetars estimated from observations [54].[3]

We get a maximum value of $\frac{dE_{GW}}{df}|_{f=f_{fmode}} = 2.5 \times 10^{37}$ ergs and a total $E_{GW} = 5.0 \times 10^{37}$ erg.

Utilising fitting relations from alternative general relativistic magnetohydrodynamic simulations reported in [19] yields comparable energy estimates $E_{GW} = 4.7 \times 10^{37}$ erg. This value is slightly smaller than that obtained using the analytic expression from [18], implying our results throughout this paper are somewhat conservative with respect to the choice of these simulations.

IV. DETECTABILITY WITH 3G DETECTORS

Current estimates of the magnetic field strength of magnetars predict values $\sim(10^{14}–10^{15})$ G [55–57]. We plot Ω_{GW} for $B_{pole} = 10^{15}$ G, 5×10^{14} G, 2.5×10^{14} G, and 10^{14} G in Fig. (2). Note the sudden drop in Ω_{GW} below $f = f_{fmode}/(1 + z_{max}) = 209.2$ Hz and beyond $f = f_{fmode} = 1883.1$ Hz. The total GW energy density Ω_{GW} varies significantly with B_{pole}. As one can see from Eqs. (7)–(10), a decrease of one order of magnitude in B_{pole} results in a decrease of almost six orders of magnitude in Ω_{GW}. We see that a value of $B_{pole} = 10^{15}$ G yields a maximum value $\Omega_{GW} \sim 10^{-21}$, which is an extremely small value compared to sensitivity estimates for third-generation gravitational-wave detectors.

The calculated signal is too weak to be detected by second-generation (2g) detectors. Even considering the combined aLIGO + aVirgo + KAGRA network, the threshold for detection is $\Omega_{GW} \sim 10^{-9}$ [58]. LISA's high sensitivity lies in a low frequency range up to $f = 10^{-1}$ Hz [59], far below the range where our signal peaks. Thus, we only consider 3g detectors, ET [22] (a triangle-shaped detector made up of three interferometers) and CE [23] (an L-shaped interferometer). We compare the strength of our
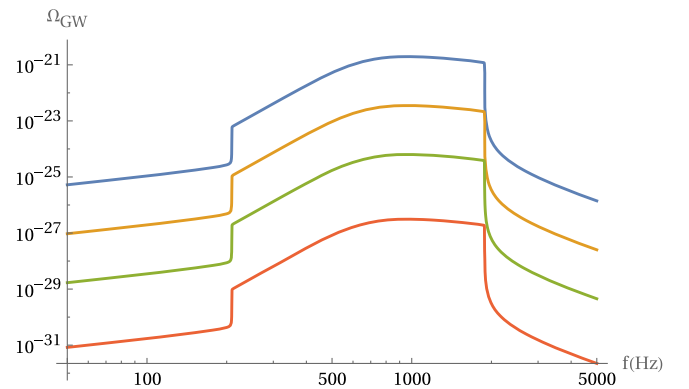

FIG. 2. The normalized GW energy spectrum of the magnetar GW background for $\lambda = 0.02539 M_\odot^{-1}$ and $B_{pole} = 10^{15}$, 5×10^{14}, 2.5×10^{14}, 10^{14} G (blue, yellow, green and red curve respectively). Cosmic expansion leads to the Doppler shifting of the f_{fmode} peak from $f = f_{fmode}$ to $f = f_{fmode}/z_{max}$, in accordance with the SFR. The contributions for frequencies outside this range are significantly lower.

---

[2]We clarify that in Eq. (10), $h(t)$ is actually taken as a step function equal to 0 in the interval $(-\infty, 0)$ and given by Eq. (9) in the interval $[0, +\infty)$, otherwise the integral in Eq. (10) is divergent.

[3]Information on known galactic magnetars can be found at http://www.physics.mcgill.ca/~pulsar/magnetar/main.html.
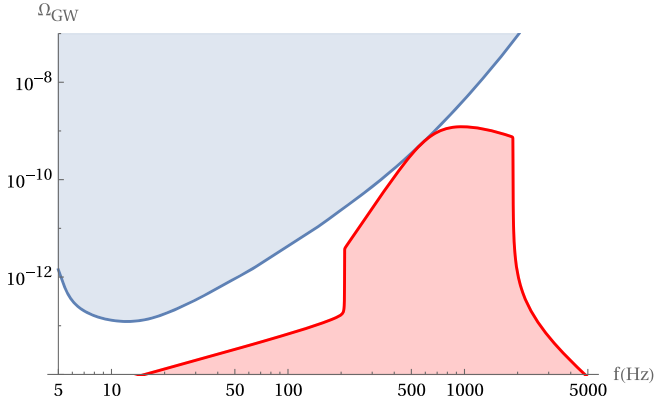
FIG. 3.   Blue curve: Ω_{GW} sensitivity of the ET + 2CE network obtained via power-law integration for one year of coherent observations. Red curve: Ω_{GW} of the magnetar GW background for $\lambda = 1 M_\odot^{-1}$ and $B_{\mathrm{pole}} = 5.7 \times 10^{16}$ G. The blue and red shaded regions need to overlap so that the signal can be detected; in this case, it is barely detectable, at frequency $f = 580$ Hz.

signal to a network of one ET and two CE detectors. The sensitivity curves for the networks of 2g and 3g detectors are obtained using power-law integration [60]; see the Appendix for a detailed explanation on the example of ET + 2CE.

Current estimates of $\sim(10^{14}$–$10^{15})$ G [55–57] for the magnetic field strength of magnetars are limited to their surface, while there is still a big uncertainty about the strength of the magnetic field in the magnetars' interior, which could reach values as high as $(10^{16}$–$10^{17})$ G [e.g., [61–63]]. For our reference value of $\lambda = 0.025 M_\odot^{-1}$, the minimum required B_{pole} for detection by the ET + 2CE network is 1.1×10^{17} G. For $B_{\mathrm{pole}} \sim 5 \times 10^{16}$ G, detection requires $\lambda \geq 2.2 M_\odot^{-1}$. Assuming that the ratio of stars turning into magnetars is $\sim 10^{-2}$ and that every magnetar emits $\sim 10^2$ MGFs in its lifetime, so that we obtain $\lambda = 1 M_\odot^{-1}$, leads to $B_{\mathrm{pole}} \geq 5.7 \times 10^{16}$ G. This is the best compromise of high values for λ and B_{pole}. Further reducing B_{pole} to $10^{16} G$ requires $\lambda \geq 2.5 \times 10^4 M_\odot^{-1}$, an unrealistically high value. In all cases, a signal that would barely be detected would be observed at $f = 580$ Hz (for our specific choice for the equation of state)—this is the frequency that offers the best chances of detection. We illustrate in Fig. 3 the requirement for detection of the produced Ω_{GW} from the ET + 2CE network. It is clear that magnetic fields of $(10^{14}$–$10^{15})$ G that match estimates for the surface strength require completely unrealistic values for λ.

V. CONCLUSIONS

We study the GW background resulting from giant magnetar flares throughout the Universe. Unlike previous studies focusing on the steady emission of GWs from non-zero stellar ellipticities [e.g., [33–37]], we explore the

effect of MGFs on the GW background. We use analytic expressions for the GW strain and energy obtained from general relativistic magnetohydrodynamic simulations of highly magnetized neutron stars. We consider a typical equation of state of $M = 1.4\ M_\odot$ and $R = 13$ km for the magnetar population. We also ignore the delay time between the star formation and the emission of MGFs, an approximation motivated by the short evolution time between star birth and supernovae as well as the young age of magnetars. There are large uncertainties in the values of the magnetic field at the pole B_{pole} and the scale factor between the MGF rate and the SFR λ. We explore these parameters in our analysis and find they significantly affect the estimate of the MGF GW background.

We conclude that the detection of the GW background from MGFs is unlikely with current or even next-generation gravitational-wave detectors. For the aforementioned choice of parameters, a number of MGFs per magnetar $\gtrsim 10^2$ (so that $\lambda \gtrsim 1 M_\odot^{-1}$) and a magnetic field $B_{\mathrm{pole}} \gtrsim 6 \times 10^{16}$ G are required for detection by the network of one ET and two CE detectors. For lower values of B_{pole}, the normalized energy spectrum falls many orders of magnitude, far lower than the sensitivity of any detector. Although we assume all magnetars to have the same properties (B field, mass, radius), taking a population distribution of these values is unlikely to significantly alter our qualitative conclusion that the background is not detectable. One could further consider other magnetic-field topologies, such as toroidal or twisted-torus magnetic fields, but we do not expect this to have a significant effect on our results. More data on the MGF rate and the strength of the magnetic field in the interior of magnetars would also prove insightful, although we are pessimistic that they would significantly alter our conclusions.

We stress that our conclusions are limited to the gravitational-wave background from MGFs. Other mechanisms may lead to a detectable gravitational-wave background from magnetars. For example, studies of GW emission due to nonzero stellar ellipticities from internal magnetic fields [e.g., [33–37]] estimate that the gravitational-wave background is detectable by 3g interferometers, although these results depend on a number of assumptions in the models that are currently not well understood.

There is still much uncertainty about the GW energetics of MGFs, and there are a number of magnetars (~ 30 currently known [54]) within/next to our galaxy. These remain a source of interest for gravitational-wave searches from individual bursts (such as [31]) with the current generation of gravitational-wave observatories.

APPENDIX: DUTY CYCLE AND SENSITIVITY CURVES

If there are enough GW events, the time between events will tend to be small compared to the duration of individual events and the overlapping signals will create a continuous background determined by the signals' spectral properties [36]. We can evaluate if MGFs are likely to form such a background by calculating the duty cycle [64] (the ratio of the duration of a typical event to the mean time between events [36]) describing a GW signal from an MGF:

$$D = \int_0^{z_{max}} R_{MGF}(z)\tau(1+z)dz, \qquad (A1)$$

where $1+z$ rescales τ to incorporate time dilation. For our conservative choice of $\lambda = 0.025 M_\odot^{-1}$, we find $D \simeq 40 \gg 1$; the GW signals are expected to form a continuous GW background signal ideal for detection using cross-correlation.

To obtain the Ω_{GW} sensitivity curve for the ET + 2CE network, we perform a cross correlation of ET placed at the Virgo site and two CE detectors located at LIGO Hanford and Livingston. We calculate the variance for the cross correlation spectrum of two interferometers [40]

$$\sigma_{IJ}^2(f) \approx \frac{1}{2T\Delta f} \frac{P_I(f)P_J(f)}{\gamma_{IJ}^2(f)S_0^2(f)}, \qquad (A2)$$

where T is the observation time, which we set at 1 yr, $\Delta f = 0.25$ Hz is the frequency resolution, $P_I(f)$ is the one-sided power spectral density of the Ith detector and is simply obtained as the square of the effective strain noise h_{eff} of the detector (see [65] for ET and [66] for CE), γ_{IJ} is the normalized overlap reduction function for the cross correlation of the Ith and Jth detector [38] and $S_0(f) = (3H_0)^2/(10\pi^2 f^3)$ [67].

We calculate $\sigma_{IJ}(f)$ for the ten different pairs resulting from the five interferometers (ET is made up of three interferometers and each CE consists of one). The total variance is

$$\sigma_{total} = \left(\sum_I^5 \sum_{J>I} \frac{1}{\sigma_{IJ}}\right)^{-1}. \qquad (A3)$$

One can obtain a sensitivity curve from σ_{total} assuming that the normalized GW energy spectrum follows a power law [60],

$$\Omega_{GW}(f) = \Omega_\beta \left(\frac{f}{f_{ref}}\right)^\beta, \qquad (A4)$$

and performing integration for a range of exponents β. We utilize a publicly available code for this process [68], considering a reference frequency $f_{ref} = 25$ Hz.

[1] Ramandeep Gill and Jeremy S. Heyl, On the trigger mechanisms for soft gamma-ray repeater giant flares, Mon. Not. R. Astron. Soc. **407**, 1926 (2010).

[2] G. L. Israel, T. Belloni, L. Stella, Y. Rephaeli, D. E. Gruber, P. Casella, S. Dall'Osso, N. Rea, M. Persic, and R. E. Rothschild, The discovery of rapid x-ray oscillations in the tail of the SGR 1806-20 hyperflare, Astrophys. J. **628**, L53 (2005).

[3] Sandro Mereghetti, The strongest cosmic magnets: Soft gamma-ray repeaters and anomalous x-ray pulsars, Astron. Astrophys. Rev. **15**, 225 (2008).

[4] Kostas D. Kokkotas and Bernd G. Schmidt, Quasi-normal modes of stars and black holes, Living Rev. Relativity **2**, 2 (1999).

[5] Yuri Levin and Maarten van Hoven, On the excitation of f modes and torsional modes by magnetar giant flares, Mon. Not. R. Astron. Soc. **418**, 659 (2011).

[6] L Matone and S Márka, Search algorithm for the detection of long-duration narrow-band transients in GW interferometers, Classical Quantum Gravity **24**, S649 (2007).

[7] B. Abbott et al., Search for gravitational wave radiation associated with the pulsating tail of the SGR 1806 − 20 hyperflare of 27 December 2004 using LIGO, Phys. Rev. D **76**, 062003 (2007).

[8] P Kalmus, R Khan, L Matone, and S Márka, Search method for unmodeled transient gravitational waves associated with SGR flares, Classical Quantum Gravity **24**, S659 (2007).

[9] B. Abbott, R. Abbott, R. Adhikari, P. Ajith, B. Allen, G. Allen, R. Amin, S. B, Anderson, W. G. Anderson, M. A. Arain, M. Araya, H. Armandula et al., Search for Gravitational-Wave Bursts from Soft Gamma Repeaters, Phys. Rev. Lett. **101**, 211102 (2008).

[10] B. Abbott et al., Implications for the origin of GRB 070201 from LIGO observations, Astrophys. J. **681**, 1419 (2008).

[11] Peter Kalmus, Search for gravitational wave bursts from soft gamma repeaters, Ph.D. thesis, 2009.

[12] J. Abadie *et al.*, Implications for the origin of GRB 051103 from LIGO observations, Astrophys. J. **755,** 2 (2012).

[13] David Murphy, Maggie Tse, Peter Raffai, Imre Bartos, Rubab Khan, Zsuzsa Márka, Luca Matone, Keith Redwine, and Szabolcs Márka, Detecting long-duration narrow-band gravitational wave transients associated with soft gamma repeater quasiperiodic oscillations, Phys. Rev. D **87,** 103008 (2013).

[14] A. Macquet, M. A. Bizouard, E. Burns, N. Christensen, M. Coughlin, Z. Wadiasingh, and G. Younes, Search for long-duration gravitational-wave signals associated with magnetar giant flares, Astrophys. J. **918,** 80 (2021).

[15] Alessandra Corsi and Benjamin J. Owen, Maximum gravitational-wave energy emissible in magnetar flares, Phys. Rev. D **83,** 104014 (2011).

[16] Burkhard Zink, Paul D. Lasky, and Kostas D. Kokkotas, Are gravitational waves from giant magnetar flares observable?, Phys. Rev. D **85,** 024030 (2012).

[17] K. Ioka, Magnetic deformation of magnetars for the giant flares of the soft gamma-ray repeaters, Mon. Not. R. Astron. Soc. **327,** 639 (2001).

[18] Paul D. Lasky, Burkhard Zink, and Kostas D. Kokkotas, Gravitational waves and hydromagnetic instabilities in rotating magnetized neutron stars, arXiv:1203.3590.

[19] Riccardo Ciolfi and Luciano Rezzolla, Poloidal-field instability in magnetized relativistic stars, Astrophys. J. **760,** 1 (2012).

[20] S. L. Detweiler, A variational calculation of the fundamental frequencies of quadrupole pulsation of fluid spheres in general relativity, Astrophys. J. **197,** 203 (1975).

[21] P. N. McDermott, H. M. van Horn, and C. J. Hansen, Non-radial oscillations of neutron stars, Astrophys. J. **325,** 725 (1988).

[22] M. Punturo, M. Abernathy, F. Acernese, B. Allen, N. Andersson, K. Arun *et al.*, The Einstein telescope: A third-generation gravitational wave observatory, Classical Quantum Gravity **27,** 194002 (2010).

[23] B. P. Abbott, R. Abbott, T. D. Abbott, M. R. Abernathy, K. Ackley *et al.*, Exploring the sensitivity of next generation gravitational wave detectors, Classical Quantum Gravity **34,** 044001 (2017).

[24] Anna L. Watts and Tod E. Strohmayer, Neutron star oscillations and QPOS during magnetar flares, Adv. Space Res. **40,** 1446 (2007).

[25] S. K. Lander and D. I. Jones, Oscillations and instabilities in neutron stars with poloidal magnetic fields, Mon. Not. R. Astron. Soc. **412,** 1730 (2011).

[26] P. Kalmus, K. C. Cannon, S. Márka, and B. J. Owen, Stacking gravitational wave signals from soft gamma repeater bursts, Phys. Rev. D **80,** 042001 (2009).

[27] B. P. Abbott *et al.*, Stacked search for gravitational waves from the 2006 SGR 1900 + 14 STORM, Astrophys. J. **701,** L68 (2009).

[28] J. Abadie, B. P. Abbott, R. Abbott, M. Abernathy, T. Accadia, F. Acernese, C. Adams, R. Adhikari, C. Affeldt, B. Allen, G. S. Allen, E. Amador Ceron *et al.*, Search for gravitational wave bursts from six magnetars, Astrophys. J. **734,** L35 (2011).

[29] Ryan Quitzow-James, Search for long-duration transient gravitational waves associated with magnetar bursts during LIGO's sixth science run, Ph.D. thesis, 2016.

[30] Ryan Quitzow-James, James Brau, James A. Clark, Michael W. Coughlin, Scott B. Coughlin, Raymond Frey, Paul Schale, Dipongkar Talukder, and Eric Thrane, Exploring a search for long-duration transient gravitational waves associated with magnetar bursts, Classical Quantum Gravity **34,** 164002 (2017).

[31] B. P. Abbott, R. Abbott, T. D. Abbott, S. Abraham, F. Acernese, K. Ackley, C. Adams, R. X. Adhikari, V. B. Adya, C. Affeldt, M. Agathos *et al.*, Search for transient gravitational-wave signals associated with magnetar bursts during Advanced LIGO's second observing run, Astrophys. J. **874,** 163 (2019).

[32] Paul Schale, Search for gravitational waves from magnetars during Advanced LIGO's second observing run, Ph.D. thesis, 2019.

[33] Tania Regimbau and Jose Pacheco, Gravitational wave background from magnetars, Astron. Astrophys. **447,** 1 (2005).

[34] T. Regimbau and V. Mandic, Astrophysical sources of a stochastic gravitational-wave background, Classical Quantum Gravity **25,** 184018 (2008).

[35] Stefania Marassi, Riccardo Ciolfi, Raffaella Schneider, Luigi Stella, and Valeria Ferrari, Stochastic background of gravitational waves emitted by magnetars, Mon. Not. R. Astron. Soc. **411,** 2549 (2011).

[36] Cheng-Jian Wu, Vuk Mandic, and Tania Regimbau, Accessibility of the stochastic gravitational wave background from magnetars to the interferometric gravitational wave detectors, Phys. Rev. D **87,** 042002 (2013).

[37] Sourav Roy Chowdhury and Maxim Khlopov, The stochastic gravitational wave background from magnetars, Universe **7,** 381 (2021).

[38] Bruce Allen and Joseph D. Romano, Detecting a stochastic background of gravitational radiation: Signal processing strategies and sensitivities, Phys. Rev. D **59,** 102001 (1999).

[39] N. Aghanim, Y. Akrami, M. Ashdown, J. Aumont, C. Baccigalupi, M. Ballardini, A. J. Banday, R. B. Barreiro, N. Bartolo *et al.*, Planck 2018 results, Astron. Astrophys. **641,** A6 (2020).

[40] R. Abbott, T. D. Abbott, S. Abraham, F. Acernese, K. Ackley, A. Adams, C. Adams, R. X. Adhikari *et al.*, Upper limits on the isotropic gravitational-wave background from Advanced LIGO and Advanced Virgo's third observing run, Phys. Rev. D **104,** 022004 (2021).

[41] Stellar Lifetimes, http://hyperphysics.phy-astr.gsu.edu/hbase/Astro/startime.html.

[42] S. Dall'Osso, J. Granot, and T. Piran, Magnetic field decay in neutron stars: from soft gamma repeaters to 'weak-field magnetars', Mon. Not. R. Astron. Soc. **422,** 2878 (2012).

[43] S. Mereghetti, Pulsars and magnetars, Braz. J. Phys. **43,** 356 (2013).

[44] P. Beniamini, K. Hotokezaka, A. van der Horst, and C. Kouveliotou, Formation rates and evolution histories of magnetars, Mon. Not. R. Astron. Soc. **487,** 1426 (2019).

[45] T. Mondal, The life cycle of magnetars: A novel approach to estimate their ages, Astrophys. J. Lett. **913,** L12 (2021).

[46] Sandro Mereghetti, Pulsars and magnetars, Braz. J. Phys. **43,** 356 (2013).

[47] Tushar Mondal, The life cycle of magnetars: A novel approach to estimate their ages, Astrophys. J. Lett. **913,** L12 (2021).

[48] Piero Madau and Mark Dickinson, Cosmic star-formation history, Annu. Rev. Astron. Astrophys. **52,** 415 (2014).

[49] Ricardo Heras, The magnetar origin of pulsars, arXiv:1104 .5060.

[50] E. Burns, D. Svinkin, K. Hurley, Z. Wadiasingh, M. Negro, G. Younes, R. Hamburg, A. Ridnaia, D. Cook, S. B. Cenko *et al.*, Identification of a local sample of gamma-ray bursts consistent with a magnetar giant flare origin, Astrophys. J. Lett. **907,** L28 (2021).

[51] G. Raaijmakers, S. K. Greif, T. E. Riley, T. Hinderer, K. Hebeler, A. Schwenk, A. L. Watts, S. Nissanke, S. Guillot, J. M. Lattimer, and R. M. Ludlam, Constraining the dense matter equation of state with joint analysis of NICER and LIGO/Virgo measurements, Astrophys. J. **893,** L21 (2020).

[52] G. Raaijmakers, S. K. Greif, K. Hebeler, T. Hinderer, S. Nissanke, A. Schwenk, T. E. Riley, A. L. Watts, J. M. Lattimer, and W. C. G. Ho, Constraints on the dense matter equation of state and neutron star properties from nicer's mass-radius estimate of PSR $j0740 + 6620$ and multimessenger observations, Astrophys. J. Lett. **918,** L29 (2021).

[53] N. Andersson and K. D. Kokkotas, Towards gravitational wave asteroseismology, Mon. Not. R. Astron. Soc. **299,** 1059 (1998).

[54] S. A. Olausen and V. M. Kaspi, The McGill magnetar catalog, Astrophys. J. Suppl. Ser. **212,** 6 (2014).

[55] Tolga Güver, Ersin Göğüş, and Feryal Özel, A magnetar strength surface magnetic field for the slowly spinning down SGR $0418 + 5729$, Mon. Not. R. Astron. Soc. **418,** 2773 (2011).

[56] Konstantinos N. Gourgouliatos, Toby S. Wood, and Rainer Hollerbach, Magnetic field evolution in magnetar crusts through three-dimensional simulations, Proc. Natl. Acad. Sci. U.S.A. **113,** 3944 (2016).

[57] Victoria M. Kaspi and Andrei M. Beloborodov, Magnetars, Annu. Rev. Astron. Astrophys. **55,** 261 (2017).

[58] Kai Schmitz, New sensitivity curves for gravitational-wave signals from cosmological phase transitions, J. High Energy Phys. 01 (2021) 097.

[59] Travis Robson, Neil J. Cornish, and Chang Liu, The construction and use of LISA sensitivity curves, Classical Quantum Gravity **36,** 105011 (2019).

[60] Eric Thrane and Joseph D. Romano, Sensitivity curves for searches for gravitational-wave backgrounds, Phys. Rev. D **88,** 124032 (2013).

[61] Kazumi Kashiyama and Kunihito Ioka, Magnetar asteroseismology with long-term gravitational waves, Phys. Rev. D **83,** 081302(R) (2011).

[62] Kotaro Fujisawa and Shota Kisaka, Magnetic field configurations of a magnetar throughout its interior and exterior— core, crust and magnetosphere, Mon. Not. R. Astron. Soc. **445,** 2777 (2014).

[63] Debarati Chatterjee, Jérôme Novak, and Micaela Oertel, Magnetic field distribution in magnetars, Phys. Rev. C **99,** 055811 (2019).

[64] Joseph D. Romano and Neil. J. Cornish, Detection methods for stochastic gravitational-wave backgrounds: A unified treatment, Living Rev. Relativity **20,** 2 (2017).

[65] S. Hild, M. Abernathy, F. Acernese, P. Amaro-Seoane, N. Andersson, K. Arun, F. Barone, B. Barr, M. Barsuglia, M. Beker *et al.*, Sensitivity studies for third-generation gravitational wave observatories, Classical Quantum Gravity **28,** 094013 (2011).

[66] LIGO-T1500293-v13: Unofficial sensitivity curves (ASD) for aLIGO, Kagra, Virgo, Voyager, Cosmic Explorer, and Einstein Telescope, https://dcc.ligo.org/LIGO-T1500293/ public.

[67] Chiara Mingarelli, Stephen Taylor, Bangalore Sathyaprakash, and Will Farr, Understanding $\omega_{gw}(f)$ in gravitational wave experiments, arXiv:1911.09745.

[68] https://git.ligo.org/kamiel.janssens/et_schumann/-/blob/ master/Data/piCurve.py.